Proceedings of The National Conference
On Undergraduate Research (NCUR) 2014
University of Kentucky, Lexington, KY
April 3-5, 2014

Pan Species Chemical Agent Detector Through Optomechanics Of Surface Acoustic Waves

Andrew Oswald
Photonics Research Center
United States Military Academy
West Point, NY 10997, USA

Faculty Advisor: John Zehnpfennig

Abstract

Present commercial and military methods of chemical detection are highly sensitized, some yield many false positives, and most require specialized training – all of which makes them impractical as deployable chemical agent detectors. Our analytical and empirical models show the possibility of detecting various pollutants in the environment by observing frequency shifts of the Brillouin acoustic mode excited on spherical or toroidal whispering gallery resonators (WGR) pumped by a telecom-wavelength evanescent field surrounding a length of tapered fiber optic cable. Due to photon-phonon interplay, the WGR experiences electrostriction, which yields both a Stokes line and Brillouin surface acoustic wave (SAW). The SAW propagates at the air-WGR interface at the speed of sound, which is determined as a weighted average of the speed of sound in the "air" material and the WGR material. Via conservation of momentum, in order to maintain resonance, the wavelength of the SAW cannot change, so a change in the speed of sound of the SAW is manifested as a change in frequency of the SAW. Therefore, a changed SAW frequency indicates that the materials through which the SAW propagates has changed. In our case, the WGR is composed of silica glass with a constant speed of sound, so a rapid shift in SAW frequency is most likely a function of a change in the "air" surrounding the WGR. Our models show it likely that we can determine the chemical agent based upon this shift in SAW frequency, and we have developed formulae based upon material properties to determine the species of chemical agent present. Here we will present our analytical and empirical methods, measurements, and results in the detection of a variety of chemical agent species.

Keywords: opto-mechanics, surface acoustic waves, Brillouin scattering

1. Introduction

Many current methods of chemical agent detection are not practical for field uses. This is of particular concern to those in the military where accurate and expedient detection of chemical agents in the environment is vital. Many chemical agent detectors provide little more than detection of a chemical agent's and fall short of identification. Chemical agent detectors walk a fine line between sensitivity, durability, and portability. As a result, many detectors can yield false positives by common pollutants in the air, require specialized training to analyze results, or are not portable enough to be used in deployed environments.

We propose the use of optical whispering gallery resonators (WGR) in a robust pan-species chemical agent detector for use in civil and military applications. Lord Rayleigh discovered the phenomenon of the acoustic

whispering gallery at St. Paul's Cathedral in 1878 [1]. Rayleigh found that acoustic waves can resonate on the outer boundary of round rooms with circumferences of integer multiples of the wavelength of the wave. The same concept applies also with optical waves.

Study in the field of surface optomechanics has led to great developments in the use of stimulated Brillouin scattering in optically coupling with WGRs to cause surface acoustic waves (SAW) [2-9]. Stimulated Brillouin scattering can cause SAWs through the evanescent coupling of optical energy from a pump on the WGR. Our analytical and empirical models show the possibility of detecting various pollutants in the environment by observing frequency shifts of the Brillouin acoustic mode excited on the spherical or toroidal whispering gallery resonators pumped by a telecom-wavelength evanescent field surrounding a length of tapered fiber optic cable. (Figure 1) shows a diagram and cutout of the fiber and WGR concept.

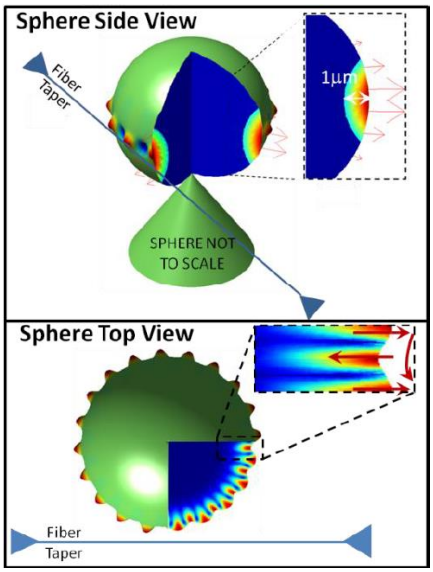

Figure 1. As light propagates through the tapered fiber, the evanescent field couples with the WGR. There is so muc h optical energy from the pump on the resonator that it forms a SAW at the air-WGR interface through photon-phon on interaction.

2. Theory

When a WGR is pumped by a laser source with a known frequency through a material transparent to the laser, optica l energy will couple onto the WGR. The optical energy from the pump on the WGR causes a SAW through electrost riction caused by photon-phonon interaction. Electrostriction causes areas of increased optical intensity to have high er density [10]. These areas of higher and lower density form the SAW. As the pump beats against the SAW, Brillou in scattering occurs as pictured in (Figure 2).

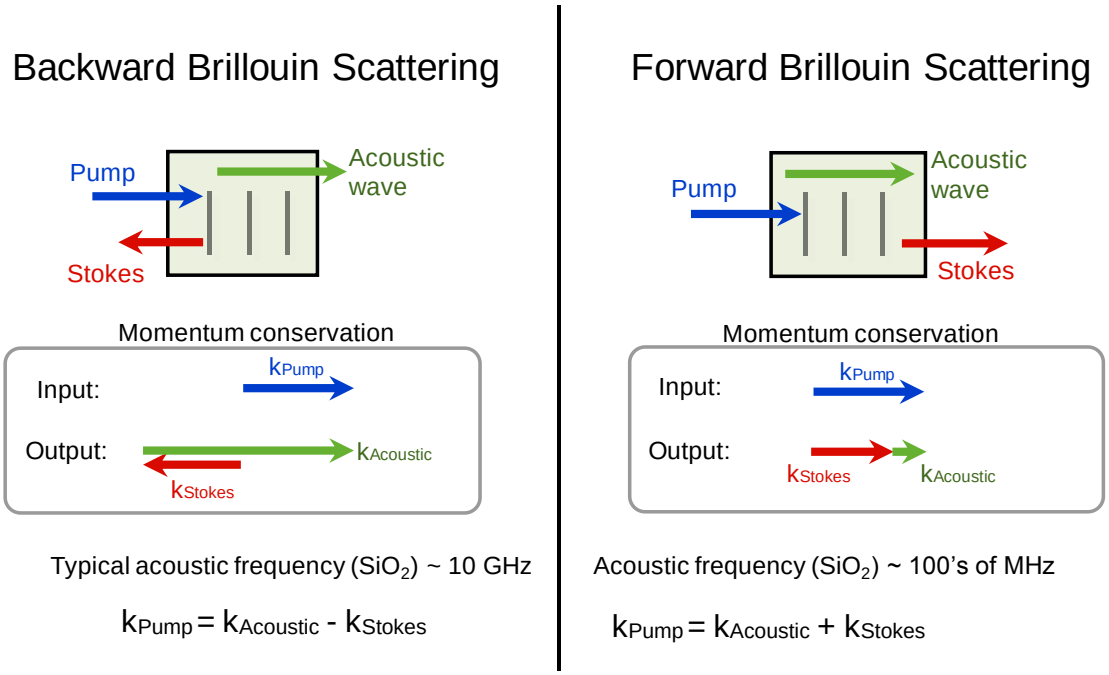

Figure 2. In Brillouin scattering the beating of an optical pump wave on an acoustic wave stimulates a red-shifted Stokes line with a frequency equal to the difference between the pump and the acoustic wave frequencies. Forward Brillouin scattering results in an acoustic wave of much lower frequency than in backward Brillouin scattering.

The acoustic wave acts as a grating for the pump so that, as the pump beats against the acoustic wave, the pumps stimulates a red-shifted Stokes line with a frequency equal to the difference between the frequencies of the pump and the acoustic wave via conservation of momentum, as seen in equation (1) where ω_s is the frequency of the optical Stokes wave, ω_p is the frequency of the optical pump wave, and Ω is the frequency of the acoustic wave.

$$\omega_s = \omega_p - \Omega \tag{1}$$

The Stokes line and the acoustic wave reinforce one another until steady state since the pump beating against the acoustic wave strengthens the Stokes line and the pump beating against the Stokes line strengthens the acoustic wave. By equation (1), the difference between ω_s and ω_p is equal to Ω. (Figure 3) shows this relationship.

To achieve resonance on the WGR, the wavelength of the SAW must be an integer multiple of the circumference of the WGR. Additionally, according to equation (2), frequency and

$$f = \frac{v}{\lambda} \tag{2}$$

speed are directly proportional to one another. The speed of sound, which is based on the density, is different for each material. As a result, v_{saw}, the speed of sound of the SAW, is ultimately dependent on both the geometry and composition of the WGR and the composition of the fluidic chemical species around the WGR. Fundamentally, we are identifying a chemical species by its density.

The SAW is the result of physical deformations on the WGR. As such, the speed of the SAW is not based solely o n either the composition of the WGR or the fluidic chemicals around the WGR. The SAW's interactions with the flu id surrounding the WGR can change ν_{saw}. This discovery led [7, 11, 12] to propose the equation:

$$\nu_{saw} = \alpha\, \nu_{bulk} + \beta\, \nu_{fluid} \tag{3}$$

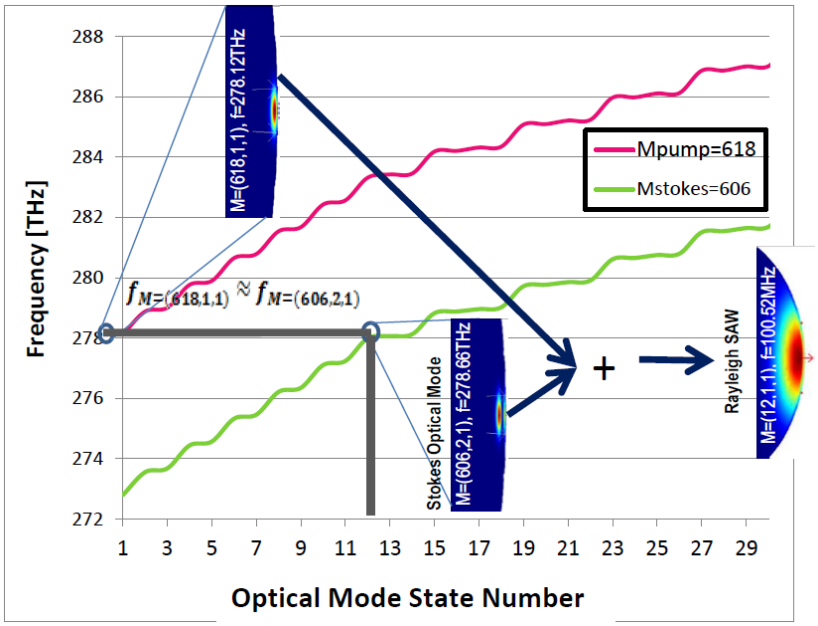

Figure 3. [9] The pump line and the Stokes line both run out to the detection system and can be measured and charac terized. The difference between the two incoming lines in energy and modal states by conservation of momentum is to be found in the SAW

which states that speed of sound of the SAW, ν_{saw}, is equal to the sum of scalar multiples (α and β) of the speed of so und in the WGR, ν_{bulk}, and the speed of sound of the fluid surrounding the WGR, ν_{fluid}. Analytic solutions for the spe ed of sound of different deformation profiles of silica glass can be found in Table 1.

In accordance with conservation of momentum, the frequency of the SAW must remain unchanged for the SAW to remain in resonance, which means the speed of sound of the SAW must also remain constant. We can attribute any c hanges in Ω, to a change in the chemical composition of the fluid surrounding the WGR. The wavelengths of both th e SAW and ν_{bulk} will remain constant because the geometry and composition of the WGR are constant. Therefore,

Table 1. Analytic solutions [12-15] and deformation profiles of most prominently observed SAW on silica WGR. Th ese values are computed for entirely planar silica-air interfaces. Actual values will be slightly different as the WGRs are spheres or toroids.

Analytic Solution on Bulk SiO_2		
Wave	**Velocity [m/s]**	**Deformation**
Longitudinal	$V_L = \left(\frac{E(\nu-1)}{\rho(2\nu^2+\nu-1)}\right)^{1/2} = 5972$	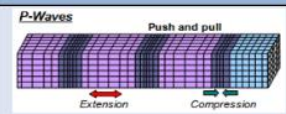
Transverse	$V_T = \left(\frac{E}{2\rho(\nu+1)}\right)^{1/2} = 3766$	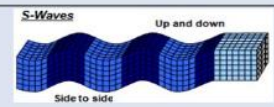
Rayleigh	$V_R = \frac{V_T(0.87+1.12\nu)}{(1+\nu)} = 3413$	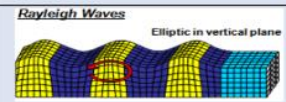

any change to ν_{saw} is a result of a change in the fluid surrounding the WGR. If we knew the exact geometry of the W GR, we could calculate the necessary pump wavelength and resulting ν_{saw}. However, since speed and frequency of a wave are directly proportional, any change in ν_{saw} will manifest as a change in Ω. We can measure both ω_s and ω_p, a nd therefore can calculate Ω and characterize any changes in ν_{saw}.

Modeling of this detection method suggests that each chemical agent has its own characteristic slope of concentrati on versus frequency of the SAW [9]. Once again, this is fundamentally based on the density, and thus speed of soun d, of the chemical species. (Figure 4) shows these results. Modeling for these characteristic slopes is time and proces sor intensive, but empirical testing should be able to produce the same results which can be used as a reference.

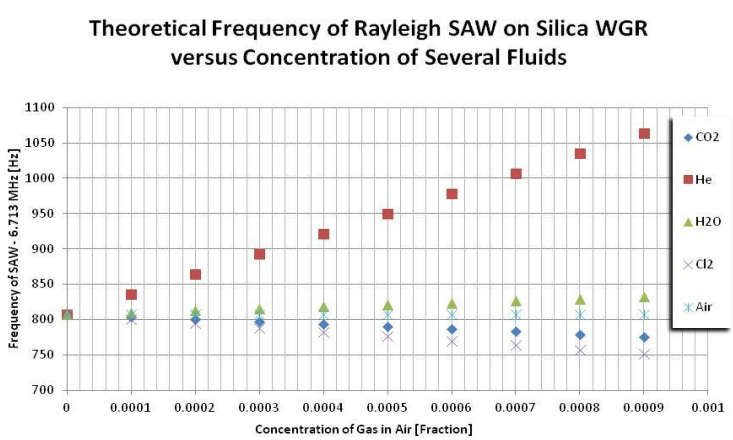

Figure 4. [9] Using known chemical and bulk properties it is possible to model probable effects of low chemical con centrations on SAW frequencies and then calculate a slope of the response. Each chemical seems to have its own ch aracteristic slope response that could be used to help predict chemical pollutants.

3. Method

The primary elements of our setup are a tunable telecom compatible laser, a circulator, single mode fiber, tapered fib er, WGR, beam combiner, oscilloscope, optical spectrum analyzer (OSA), and electrical spectrum analyzer (ESA). T hese can be seen in (Figure 5).

The tapered fiber is fiber optic cable stripped of the cladding then pulled slowly over a flame. The tapered fiber is used to access the evanescent field surrounding the fiber. Evanescent access blocks (EABs) are another common met hod of evanescent access. The pump source propagates down the single mode fiber as normal. We taper the fiber to ensure only one spatial mode of light is able to propagate through the fiber taper. At the taper, the Gaussian power pr ofile of a single mode is geometrically wider than the diameter of the fiber, so some of the electromagnetic field pro pagates through the free space outside the fiber. This is known as the evanescent field.

We place a WGR infinitesimally close to the fiber. For WGRs, we have used both spheres and toroids as seen in (Figure 6). The evanescent field decays exponentially, so positioning the WGR as close to the fiber as possible is imp erative. When enough optical power in the evanescent field couples with the WGR, there is so much optical energy f rom the pump on the resonator that it forms a SAW through photon-phonon interaction.

In the frequency domain, this resonance manifests itself as a spike in the frequency of the Stokes line on both the OSA and the ESA. The OSA also shows a spike in the SAW frequency. In the time domain, resonance manifests itse lf as a regular dramatic shift in the power profile over time (“shark tail” seen on the oscilloscope).

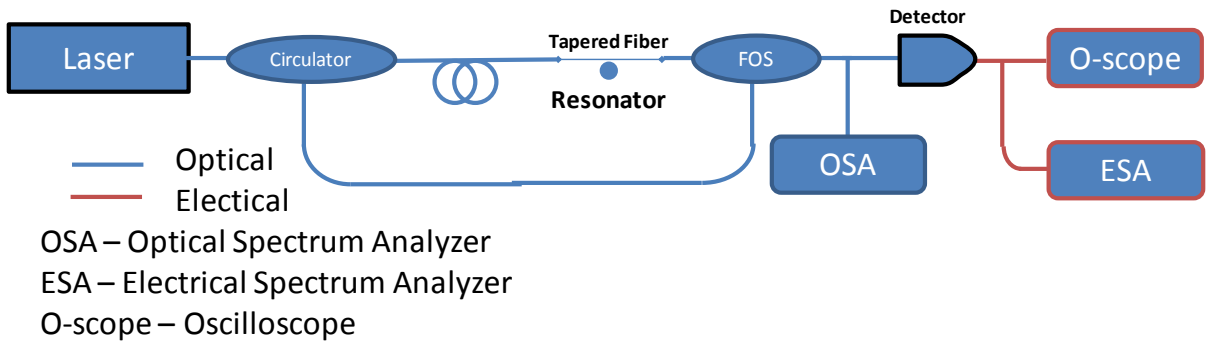

Figure 5. The experimental setup consists of a tunable telecom wavelength laser, a circulator to remove and observe backward scattering, tapered fiber, WGR, beam combiner to combine backward scattering and forward scattering, oscilloscope, optical spectrum analyzer, and , electrical spectrum analyzer.

If we then change the concentration of the chemical agent present in the fluid around the WGR, we should see a sh ift in the frequency or in the "shark tail". If taken at several different concentrations, the results can be plotted and us ed to determine the characteristic slope of the chemical agent.

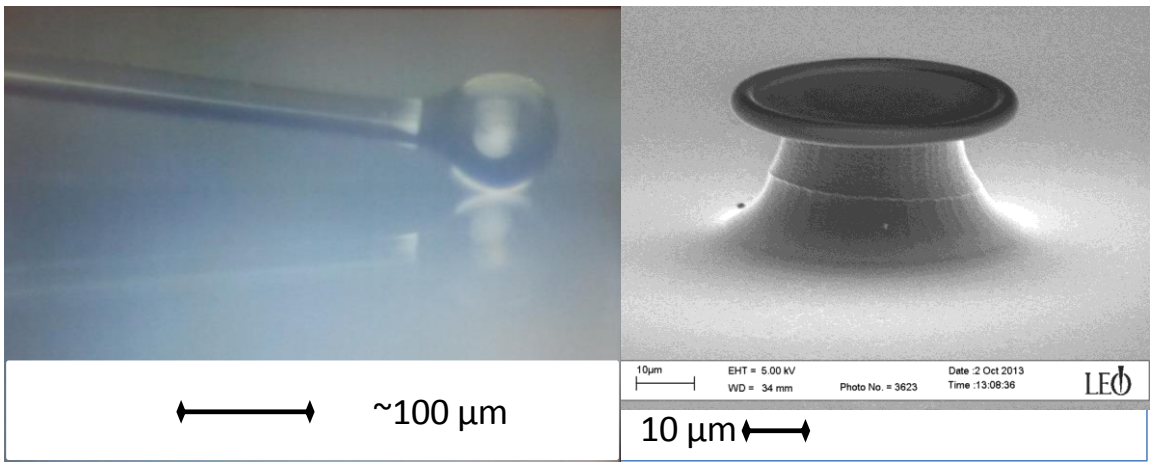

Figure 6. Sphere and toroid used as a WGR. The sphere is made from tapered fiber superheated and allowed to cool. As a result of surface tension and gravity a sphere is the shape which requires the least energy to maintain. The toroid is grown on a piece of glass in a clean room

4. Results

Prior to conducting experiments, we simulated both our tapered fiber and EAB models. (Figure 7) shows the results of both simulations. The tapered fiber simulations showed the consistent and sustainable resonance which can prove our hypothesis. The consistent pattern around the WGR correlates to areas of higher and lower optical intensity. Through electrostriction, this causes a SAW which further builds the resonance in this simulation. The simulation of the EAB, on the other hand, shows only optical energy coupling onto the resonator. Our simulation of the EAB suggests that we cannot achieve resonance the same way as with the tapered fiber. The EAB would provide more stability and consistency, but also increases the WGR's standoff from the core, reducing the power of the evanescent field. As such, we continued forward with the tapered fiber.

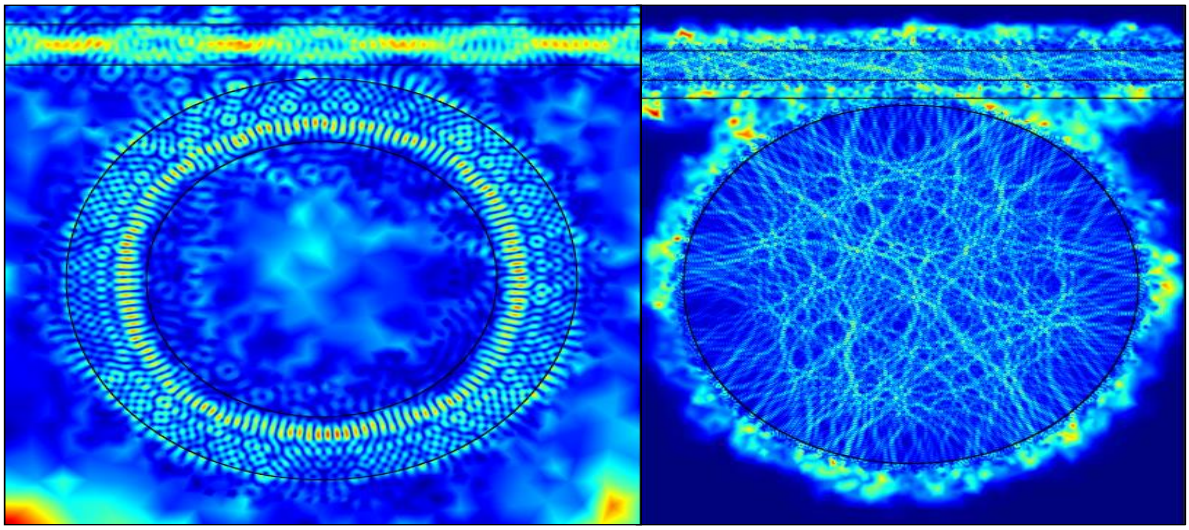

Figure 7. Simulations of tapered fiber (left) and EAB (right) with a spherical WGR. The simulation of the tapered fiber with a WGR shows strong resonance. The consistent pattern around the WGR shows areas of higher and lower optical intensity which are key to electrostriction. The EAB with a WGR shows optical energy coupling onto the resonator but no resonance.

To date we have developed and improved methods of tapering a fiber and creating spheres to use as WGRs. Both processes are time-consuming and require great finesse, yet still only yield useful products approximately one time in every five attempts. Developing these procedures and techniques has been slow and laborious but has allowed us to replicate our testing with relatively high accuracy. We have also begun to achieve resonance with WGRs.

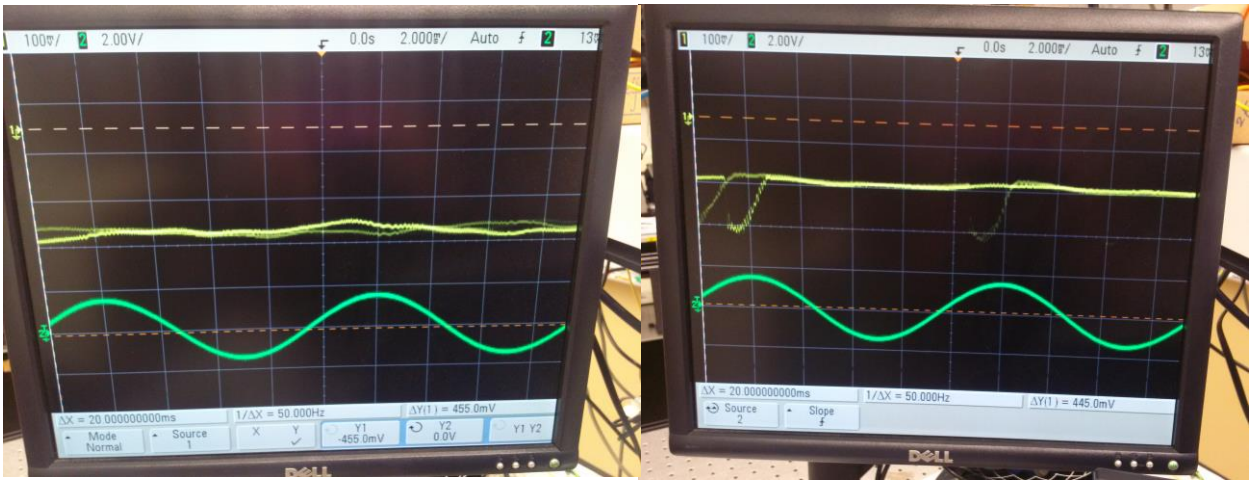

Figure 8. Beginning signs of resonance. The yellow waveform is the signal. The green waveform is the pump modulation driver. The image on the left shows the tell-tale ripple of the waveform as the SAW begins to form on the WGR. The image on the left shows the "shark tail" waveform that signals resonance is occurring.

(Figure 8) shows the waveform of a WGR hovering in and out of resonance. The power level is changing as more and less optical power is coupled out of the fiber onto the WGR. The "shark tail" waveform means a SAW has formed. When the "shark tail" is steady, the SAW has reached a steady sate. The WGR was not surrounded by any pollutants at this point, so this would serve as a baseline for detection. We were not able to maintain the resonance, so no frequency data could be taken. An interesting note is that the SAW is susceptible to interference by other acoustic waves. Clapping our hands resulted in a noticeable jump in the waveform, and even changing the pressure around the WGR and taper could affect the resonance.

This weak resonance is the first step to useable resonance and data, but we still need to accomplish more before we get consistent and reliable resonance with WGRs. We believe the fiber could be pulled to an even finer taper resulting in more of the evanescent field propagating outside the core and thus an increase of photon-phonon interaction. The WGR must also be very steady next to the fiber otherwise it will not be able to maintain resonance. Therefore, we are improving our position and support systems.

5. Conclusion

Our models show that the surface SAWs on WGRs can be used in a chemical agent detector. A pump will evanescently couple with the WGR and cause a SAW through photon-phonon interaction and produce a red-shifted Stokes line through conservation of momentum. The chemical agent present in the air around the WGR will cause a change in the speed of sound of the SAW which will result in a measurable change in frequency of the Stokes line. The slope of the frequency shift is a characteristic of the chemical agent and can be predicted. This can be used as a pan-species chemical agent detector.

6. Acknowledgements

The authors thank the Army Research Office and the Defense Advanced Research Projects Agency for their generou s support of this project.

7. References

[1] L. Rayleigh, “The problem of the whispering gallery,” *Philos. Mag.* vol. 20, no 120, pp. 1001-1004, 1910.

[2] T. Carmon, H. Rokhsari, L. Yang, T. J. Kippenberg, and K. J. Vahala, "Temporal behavior of radiation-pre ssure-induced vibrations of an optical microcavity phonon mode," *Physical Review Letters,* vol. 94, p. 2239 02, 6 2005.

[3] Q. Lin, J. Rosenberg, X. Jiang, K. Vahala, and O. Painter, "Mechanical oscillation and cooling actuated by the optical gradient force," *Physical Review Letters,* vol. 103, p. 103601, 2009.

[4] X. Jiang, Q. Lin, J. Rosenberg, K. Vahala, and O. Painter, "High-Q double-disk microcavities for cavity opt omechanics," *Opt. Express,* vol. 17, pp. 20911-20919, 11/09 2009.

[5] M. Tomes and T. Carmon, "Photonic micro-electromechanical systems vibrating at X-band (11-GHz) rates, " *Physical Review Letters,* vol. 102, p. 113601, 2009.

[6] G. Bahl, X. Fan, and T. Carmon, "Acoustic whispering-gallery modes in optomechanical shells," ed.

[7] J. Zehnpfennig, "Surface Optomechanics: Forward and Backward Scattered Surface Acoustic Waves in Sili ca Microsphere," Masters of Science in Engineering (Electrical Engineering) Written in University of Mich igan, Ann Arbor's Rackham Graduate School Doctoral Dissertation format, Electrical Engineering and Co mputer Science, University of Michigan, Ann Arbor, ProQUEST, 2011.

[8] G. Bahl, J. Zehnpfennig, M. Tomes, and T. Carmon, "Stimulated optomechanical excitation of surface acou stic waves in a microdevice," *Nature Communications,* vol. 2, p. 6, 26 July 2011 2011.

[9] D. Covell, M. Letarte, “Use of Surface Acoustic Waves in Whispering Gallery Resonators for a Pan-Specie s Chemical Detector,” presented at the National Conference of Undergraduate Research 2013, La Crosse, WI, 2013.

[10] R. W. Boyd, *Nonlinear optics.* San Diego, CA: Academic Press, 2003.

[11] J. Zehnpfennig, M. Letarte, R. W. Sadowski, and J. J. Raftery Jr., "Surface Optomechanics: Calculation of Love Surface Acoustic Waves on Microresonators," presented at the Conference on Lasers and Electro Opti cs 2012, San Jose, CA, 2012.

[12] J. Zehnpfennig, M. Letarte, D. Covell, K. E. Sheetz, and J. J. Raftery Jr., "Surface Optomechanics: Analyti c Solution of Detection Limits of Surface Acoustic Waves in Various Fluids," presented at the Frontiers in Optics 2012, Rochester, NY, 2012.

[13] L. Kinsler, A. Frey, A. Coppens, and J. Sanders, "Fundamentals of acoustics," 1999.

[14] D. S. Ballantine and Knovel, Acoustic wave sensors: theory, design, and physico-chemical applications. Sa n Diego: Academic Press, 1997.

[15] Pham Chi Vinh and P. G. Malischewsky, "Improved Approximations of the Rayleigh Wave Velocity," Jour nal of Thermoplastic Composite Materials, vol. 21, pp. 337-352, July 1, 2008 2008